

# A Molecular Index for Biological Age identified from the Metabolome and Senescence-associated Secretome in Humans

**Shruthi Hamsanathan**

Aging Institute, University of Pittsburgh

**Tamil Anthonymuthu**

Department of Critical Care Medicine, University of Pittsburgh <https://orcid.org/0000-0002-3460-5003>

**Denise Prosser**

Department of Medicine, University of Pittsburgh

**Anna Lokshin**

Department of Medicine, University of Pittsburgh

**Susan Greenspan**

Division of Geriatric Medicine, University of Pittsburgh

**Neil Resnick**

Division of Geriatric Medicine, University of Pittsburgh

**Subashan Perera**

Division of Geriatric Medicine, University of Pittsburgh

**Giri Narasimhan**

Florida International University <https://orcid.org/0000-0003-0535-4871>

**Aditi Gurkar** (✉ [agurkar1@pitt.edu](mailto:agurkar1@pitt.edu))

Aging Institute, University of Pittsburgh <https://orcid.org/0000-0003-4338-0624>

---

## Article

**Keywords:** Biological age, metabolomics, cellular senescence, SASP, aging

**Posted Date:** August 31st, 2020

**DOI:** <https://doi.org/10.21203/rs.3.rs-62559/v1>

**License:**   This work is licensed under a Creative Commons Attribution 4.0 International License.

[Read Full License](#)

# Abstract

Unlike chronological age, biological age is a strong indicator of health risk and reflects the physiological state of an individual. However, the molecular fingerprint associated with biological age is ill-defined. To define a high-resolution molecular signature of biological age, we analyzed the metabolome, circulating senescence markers and the interaction between them during biological aging from a cohort of healthy and rapid agers. We report that the balance between two fatty acid oxidation mechanisms,  $\beta$ -oxidation and  $\omega$ -oxidation, determines the extent of healthy aging. Furthermore, a panel of 18 metabolites, Healthy Aging Metabolic (HAM) index, can predict healthy agers regardless of gender, smoking and race (ROC\_AUC = 0.95). Although not the best predictor of biological age, rapid agers have elevated levels of MCP-1, Cystatin C, CRP and IL-6. Our findings indicate that biological age is associated with a network of metabolic processes. Hence, intervention strategies to improve healthspan should target multiple metabolic pathways.

## Introduction

Aging is a complex biological process often defined as a progressive loss in physiological function over time. Epigenetic, genetic, environmental and lifestyle factors can all impact the aging process and therefore individuals with similar lifespans exhibit varying levels of physiological function<sup>1</sup>. Thus, chronological age (years since birth) is a poor measure of the rate of aging in an individual. In this context, the biological age, which reflects the functional ability and the state of health of an individual may act as a better measure of aging<sup>2</sup>. Therefore, understanding biological aging is the key to improve and preserve the health and quality of life of older adults. A number of studies have identified signals that measure aging in general, with an attempt to reflect biological age. Candidate markers for biological aging measures include individual phenotypic parameters such as low-grade inflammation, muscle mass and strength, frailty, neuroendocrine function and immune markers<sup>3-6</sup>. While these markers are successful in depicting the individual events in the aging process, they do not truly represent the complexity of biological aging.

The use of molecular signatures as potential indicators to accurately predict the risk of age-related diseases and mortality has gained a lot of interest. In this light, several DNA methylation clocks based on CpG methylation rates have been established to represent epigenomic aspects of the aging process<sup>7,8</sup>. Such clocks have strong predictive abilities. The second-generation clocks, PhenoAge and GrimAge, integrate DNA methylation profiles with clinical biomarkers and are predictive of mortality and age-related diseases<sup>9,10</sup>. The shortening of telomere length has also been used for predicting chronological age<sup>11</sup>. Recently, use of artificial intelligence (AI) has been gaining popularity for integrating aging clocks. For example, deep learning clocks based on transcription signatures from muscle-tissues provided target candidates for pharmaceutical intervention in sarcopenia<sup>12</sup>. Similarly, a plasma proteomics clock was developed using 373 age-associated proteins<sup>13</sup>. However, clear associations between the aging proteome and environmental factors could not be identified.

Although the ‘clocks’ mentioned above have provided a deeper insight into aging, gaps exist in our understanding of biological age. For example, the rationale behind the mechanism of DNA methylation that forms the basis of epigenetic clocks still remains unclear. In addition, most of these indicators are trained with chronological age and undermine the differences between predicted and chronological age impacting the overall sensitivity<sup>14</sup>. Disentangling chronological age from biological age is quite challenging and necessitates a complex experimental design right from careful selection of cohorts to employing high-resolution approaches to predict high-accuracy composite markers.

Metabolomics is a powerful tool that has the ability to capture the complete set of metabolites produced and is particularly suited to account for biological aging. One potential advantage of metabolomics over other ‘omic’ approaches is that metabolites are the final downstream products and changes are more closely related to the immediate (patho)physiologic state of an individual. The dimensionality of metabolites in capturing both genetic and non-genetic features often influenced by disease, environment, microbiome and lifestyle factors makes it an ideal candidate for measuring a complex process such as aging<sup>15</sup>. Furthermore, a number of interventions that have shown some promise and are directed to improve healthspan, such as calorie restriction, time-restricted feeding, and intermittent fasting are known to target metabolic pathways<sup>16–18</sup>. Metabolomic profiling is also advantageous over the widely studied DNA and protein-based clocks because they provide information on metabolic pathways in addition to biomarkers predicting age-related morbidity, which could be further explored to tailor interventions.

In addition to metabolomic alterations, changes in senescence-associated inflammatory markers are another important but underexplored drivers of biological age. When cells encounter stochastic macromolecular damage or stress, they can enter a state of permanent cell cycle arrest known as senescence<sup>19,20</sup>. It is evident that there is an increase in the number of senescent cells with age. These senescent cells primarily secrete multiple inflammatory cytokines and elicit low-grade inflammation. This pro-inflammation status leads to subsequent age-related diseases and morbidity<sup>21</sup>. Indeed, modulation of secretory pathways and clearance of senescent cells has emerged as an attractive therapeutic strategy for aging<sup>22,23</sup>. However, translation to human applications is impeded by the fact that we do not know how prevalent senescent cells are *in vivo* and whether these cells promote biological aging in humans. Although the senescence associated secretory phenotype (SASP) secretome is thought to be a major contributor to aging pathology many of the SASP cytokines individually have also been associated with stress, pathogenic infection and other non age-related diseases. Therefore, none of the currently available markers are sufficient on their own for conclusively identifying the burden of senescent cells.

While there is some evidence for metabolic changes and inflammation with chronological age, do these changes contribute to either rapid biological aging or healthy aging is unclear. Early identification of accelerated biological age is critical for clinical decisions in order to delay the onset of age-related diseases, increase well-being and reduce healthcare costs. Identifying the unique molecular markers responsible for early biological aging would be crucial for understanding the biopathophysiology of the aging process and to guide appropriate intervention strategies. We adopted an integrated approach in

this study, and simultaneously measured SASP factors and metabolites from serum samples to generate a fingerprint unique to accelerated and healthy biological aging.

## Results

Biological age, not chronological age, captures one's physical and functional ability and is a determinant of *healthspan* (years lived in good health). We took an integrated approach encompassing high-resolution metabolomics combined with a panel of SASP and proinflammatory markers in the serum, to define a molecular index for biological aging. Walking ability, reflects an integrated assessment of cardiovascular fitness, muscle strength, and neurological and joint function and is currently the single best predictor in humans of hospitalization, functional decline, disability, surgical complications, institutionalization and death<sup>24–27</sup>. The 'SOLVE-IT' cohort consisted of 196 total participants, 98 individuals above 75 years old that showed good walking ability (walk up a flight of stairs and walk for 15 minutes without resting). These individuals were physically active and hence classified as "healthy" agers. The remaining 98 were classified as "rapid" agers as they displayed poor walking ability despite being chronologically younger than the healthy agers<sup>28</sup> (Fig. 1a). Additionally, multiple measures such as gait, function, mental status, strength, activity and comorbidity index were included in our study. Phenotypic age is an effective predictor of overall health risks and it is strongly associated with the chronological age<sup>29</sup>. However, one of the unique features of the 'SOLVE-IT' study is that the biologically-aged individuals are readily distinguishable from chronologically-aged individuals. In this study cohort, frailty, comorbidities, impaired cognitive ability (defined by poor Montreal Cognitive Assessment scores) and higher body mass index (BMI) are negatively associated with chronological age and more prevalent in rapid agers. Such an inverse association of biological age and chronological age, as demonstrated in this cohort, offers an advantage in delineating specific signatures of healthy aging (Fig. 1b). It is to be noted that incidence of declining organ functions such as heart, kidney, and liver failures, as well as, cancer were alike in both rapid and healthy agers (Fig. 1b), thereby strengthening the unique appropriateness of the cohort for identification of markers associated with functional aging.

To define the molecular fingerprint associated with biological aging, we performed high-resolution metabolomics by Ultrahigh Performance Liquid Chromatography-Tandem Mass Spectroscopy (UPLC-MS/MS). We used serum samples for our study since it is minimally invasive, affordable, and has reduced overall risk for patients. In addition, several recent studies with heterochronic parabiosis, as well as blood/serum transfusions in animal models suggest that systemic circulating factors in blood, drives the aging phenotype<sup>30</sup>. A total of 1327 serum metabolites were identified that belonged to 9 different super pathways as defined by KEGG analysis. Majority of the identified metabolites were lipids (32%), followed by xenobiotics (17%) and amino acids (16%). The identified metabolite super pathways were further summarized into sub pathways. Long and medium-chain acylcarnitines (40), fatty acid dicarboxylate (31), sphingomyelins (29), diacylglycerols (29) and lysophospholipids (25) were predominant groups among lipids. Leucine, Isoleucine and Valine Metabolism (33), Arginine and Proline Metabolism (22), Tryptophan Metabolism (23) and Methionine, Cysteine, SAM, and Taurine Metabolism

(22) were some of the sub pathway profiles for amino acid metabolism that were identified (Fig. 1c). The inter-relationship between the identified metabolites revealed 1481 highly correlated (Spearman's  $\rho > 0.8$ ) 'metabolite pairs'. Over 200,000 significant correlations were observed among metabolite pairs, with 33,763 lipid-lipid pairs and 23,761 lipid-amino acid pairs. Interestingly, choline derivatives of long and very long-chain free fatty acids (16–22 carbons) displayed remarkably high correlations. The identified fatty acylcholines (36) had a minimum  $\rho > 0.606$ ; for example, palmitoylcholine (16:0) and steroylcholine (18:0) showed an exceptionally high correlation  $\rho = 0.94$  (Fig. 1d), suggesting a controlled acylcholine synthesis irrespective of heterogenous traits. Overall, our metabolomic analysis from this cohort generated a rich set of metabolite data that included several metabolic pathways.

### Differential metabolome pattern associated with biological age.

We used Orthogonal partial least square-discriminant analysis (OPLS-DA), a multivariate supervised classification method with 7-fold cross validation consisting of 200 iterations in each round to distinguish metabolic differences between healthy and rapid agers. OPLS-DA analysis produced a model with  $R^2$  (cumulative) = 0.76,  $Q^2$  (cumulative) = 0.40 with a predictive power of 95.9%, fisher  $p$ -value =  $1.45 \times 10^{-45}$  and a root mean square cross validation error RMSE = 0.386. The model separated healthy and rapid agers demonstrating a clear difference in the metabolome associated with biological age (Fig. 2a). To identify metabolites that are associated with healthy and rapid agers, we used receiver operative characteristic (ROC) analysis based on a logistic regression model. We noted that higher levels of some of the metabolites were predictive of healthy agers, Area Under the Curve (AUC) value for healthy aging ROC curve,  $ROC\_AUC_{HA} > 0.5$ ) and some were predictive of rapid agers (AUC value for rapid aging ROC curve,  $ROC\_AUC_{RA} > 0.5$ ). Therefore, we combined these ROC\_AUC scores to create a single variable  $AUC_{comb}$  (see methods). Metabolites with AUC values more than 0.5 were considered indicators of healthy agers while, less than 0.5 were associated with rapid agers. There were (331) metabolites that significantly distinguished healthy and rapid agers, with (125) metabolites as predictors of healthy aging and (206) as predictors of rapid aging ( $q$ -value  $< 0.05$ ) (Fig. 2b). Eicosenoylcarnitine (C20:1), an acylcarnitine was one of the most influential metabolites in discriminating healthy agers from rapid agers ( $AUC_{comb} = 0.72$ ). Beside acylcarnitines, healthy agers were also distinguished by beta-cryptoxanthin ( $AUC_{comb} = 0.70$ ), a precursor of vitamin A, important for general growth, development and immune response. Gut microbiome-metabolite, 1H-indole-7-acetic acid ( $AUC_{comb} = 0.70$ ) was also elevated in healthy agers. In contrast, dicarboxylic fatty acids (DCA) such as pimelate (C7) ( $AUC_{comb} = 0.30$ ), suberate (C8), sebacate (C10) ( $AUC_{comb} = 0.33$ ) and undecanedioate (C11) ( $AUC_{comb} = 0.31$ ) were elevated in rapid agers. Similarly, glutamate and mannose also elevated in rapid agers ( $AUC_{comb} = 0.33$ ) (Fig. 2b, **source data**).

To understand biological pathways associated with either healthy or rapid agers, we analyzed metabolites that significantly separated the two groups at  $p$ -value  $< 0.05$ , using Ingenuity Pathway Analysis (IPA). We found that Hypoxia-inducible factor 1-alpha (HIF1 $\alpha$ ) signaling, 4-hydroxyproline  
 Loading [MathJax]/jax/output/CommonHTML/jax.js tion, and citrulline metabolism were mainly associated with

accelerated biological age (Fig. 2c). Consistent with our results, other studies have shown that upregulated HIF1 $\alpha$  signaling impairs mitochondrial biogenesis and accelerates aging. Sirtuins are the main class of enzymes that destabilize HIF1 $\alpha$  thereby promoting mitochondrial health during aging<sup>31</sup>. Similar to these reports, healthy agers positively associated with sirtuin signaling pathways, generally linked to longevity (**supplementary Fig. 1**). Choline degradation, carnitine metabolism, gamma-glutamyl cycle were some of the other pathways associated with healthy agers (**supplementary Fig. 1**). In addition to general metabolic pathways, IPA was used to provide disease and biofunction predictions. Disease/injury associated metabolites were related to gastrointestinal disease, skeletal and muscular disorders, organismal injury and neurological diseases (Fig. 2D). This data suggests that certain co-morbidities may exhibit metabolic profiles which may indicate underlying conditions, although they were not clinically observed in rapid agers at the time of sample collection. Collectively, these results show that metabolites and associated pathways can differentiate healthy and rapid biological agers.

### Balance of fatty acid oxidation pathways predicts healthy agers.

Next, we sought to identify specific metabolite signatures that can serve as potential indicators for healthy aging. Acylcarnitines, especially long chain acylcarnitines and dicarboxylic acids (DCAs) were the two important classes that were identified both in the OPLS-DA and ROC analysis (Fig. 3a). Acylcarnitines play a major role in regulating lipid metabolism by shuttling fatty acids into mitochondria. Under physiological conditions, oxidation of long- and medium-chain fatty acids is primarily carried out by mitochondrial  $\beta$ -oxidation (Fig. 3b). We observed 9 acylcarnitines, mostly long chain forms with ROC\_AUC<sub>HA</sub> values 0.6–0.72 (Fig. 3a). An alternate, subsidiary pathway to  $\beta$ -oxidation is  $\omega$ -oxidation occurring in endoplasmic reticulum (ER) microsomes<sup>32</sup>.  $\omega$ -oxidation of fatty acids generates dicarboxylic fatty acids (DCAs) and is an alternate pathway used when mitochondrial  $\beta$ -oxidation is impaired (Fig. 3b). Our analysis detected 3 important DCAs: pimelate, undecanediote and suberate with ROC\_AUC<sub>RA</sub> values 0.6–0.7. In healthy agers, the acylcarnitines levels were higher than in rapid agers suggesting that  $\beta$ -oxidation is predominantly active in the former. On the other hand, rapid agers showed higher levels of DCAs compared to healthy agers indicating increased  $\omega$ -oxidation (Fig. 3a). The predictive power obtained from the difference in acylcarnitines and DCAs improved by 0.06 compared to the best individual predictor (eicosenoylcarnitine) (Fig. 3c, d). These results suggest a balance between  $\beta$ -oxidation and  $\omega$ -oxidation pathways can potentially influence biological age.

## Identification of Healthy Aging Metabolic (HAM) index

Aging is a complex process that cannot be realized through one metabolic pathway or a metabolite class. Indeed, several reports have implicated the roles of multiple pathways affecting the aging process. For example, dysregulation of the carnitine shuttle and vitamin E pathways have been associated with frailty<sup>33</sup> whereas, tryptophan metabolism, particularly, kynurenine pathway is implicated in age-related chronic inflammation and memory impairment<sup>34</sup>. Therefore, we hypothesized that a combination of metabolites from different pathways could possibly be a better molecular indicator for biological age,

rather than a single metabolite/pathway. The combinatorial approach can overcome the moderate predictive power presented by the individual metabolites. In order to identify a panel of metabolites that are better predictors of healthy biological aging we chose all known endogenous metabolites from OPLS-DA analysis with Variable Importance of the Projection (VIP) score  $> 1$  and fit a linear regression model. We used LASSO regression method with 10-fold cross validation with 1000 bootstrapping steps in each validation. LASSO regression model eliminates the collinear variables and retains only the significant variables ( $p < 0.05$ ). The final model retained a panel of 18 metabolites with a Pearson's  $r = 0.74$  and  $p < 0.0001$  (Fig. 3e). The model consisted of metabolites primarily related to fatty acid metabolism, the TCA cycle, amino acids and glutathione metabolism and strongly predicted healthy biological agers. Importantly, based on the model values we derived a healthy aging indicator "Healthy Aging Metabolic (HAM) Index". The HAM index was significantly different between the healthy agers and rapid agers ( $p < 0.0001$ ) and showed a ROC\_AUC<sub>HA</sub> value of 0.95 in identifying healthy agers (Fig. 3f, g). Compared to some of the biological age indices such as frailty index, gait speed, MOCA score (**supplementary Fig. 2**), the HAM index outperformed these indices in predicting healthy agers from rapid agers (Fig. 3h). This predictive power from a combination of metabolites points out that several different pathways are involved in maintaining a healthy biological age.

### SASP markers associated with rapid agers.

Circulating factors such as senescence-associated secretory phenotype (SASP) and pro-inflammatory markers can reflect the state of aging cells. Senescence-associated 'secretome' could be a valuable marker for aging and age-associated diseases. With this in mind, we wanted to investigate age-associated proinflammatory markers in the context of biological age. To test this we measured multi-analyte SASP markers in serum using Luminex High Performance Assay. The list of SASP and proinflammatory markers examined were based on evidence from several studies (**supplementary table 1**). Interestingly, Cystatin C and CCL-2/MCP-1 were found to be elevated in rapid agers compared to healthy agers (Fig. 4a). Serum Cystatin C belongs to the family of Cystatin protease inhibitors and consistent with our analysis, has been shown to increase significantly with age, even in the absence of clinical risk factors for renal dysfunction<sup>35</sup>. Similarly, monocyte chemoattractant protein 1 (MCP1) is a key chemokine that is important for infiltration of macrophages and monocytes. These data suggest that a subset of SASP factors track with increased biological age independent of chronological age.

Next, we examined the metabolomic profiles associated with CCL-2/MCP-1 and Cystatin C. As shown in Fig. 4c **and source data**, CCL-2/MCP-1 was associated with 57 metabolites (FDR-correlated  $p < 0.2$ ) with majority (56%) contributed by lipids, particularly, lysophospholipids (11), diacylglycerols (6) and phosphatidyl glycerol (6). In contrast to CCL-2/MCP-1, Cystatin C showed positive association with metabolites that belonged to both lipids (175) and amino acids (150) (Fig. 4d, **source data**). A panel of serum metabolites that displayed remarkable correlation with Cystatin C is shown in Fig. 4e. Interestingly, the levels of CCL-2/MCP-1 and Cystatin C levels were random among the age groups and did not influence one another as suggested from Spearman's  $\rho$  with a  $p$ -value  $> 0.05$ .

In addition to Cystatin C and CCL-2/MCP-1, C-reactive protein (CRP) and interleukin-6 (IL-6) were also elevated in rapid agers (Fig. 4b). Tryptophan (4), Tyrosine (4) metabolism, fibrinogen cleavage peptide (7), vitamin E metabolism, androgenic steroids (7) showed positive association with CRP whereas ceramides (5) were negatively associated with CRP. Cleaved fibrinogen products, as well as, higher levels of Tryptophan metabolism products such as kynurenine and indole-3-carboxylates suggest chronic inflammation in rapid agers (**supplementary table 2**). Metabolites associated with IL-6, particularly DSGEGDFXAEGGGVR, Fibrinopeptide B (1–13), ADSGEGDFXAEGGGVR and Fibrinopeptide A (3–16) also support the prevalence of a low-grade inflammation with accelerated biological age<sup>36</sup>.

In order to understand the relationship between metabolites/metabolic pathways and circulating secretory factors in aging, we looked for common metabolites that were associated with secretory factors and biological age groups. Five classes of metabolites- acylcarnitine, oleoyl/linoleoyl glycerol phosphocholine, carotene diol,  $\gamma$ -glutamyl glutamine and nicotinamide that were strongly associated with healthy aging were found to be negatively associated with Cystatin C, MCP-1, CRP, as well as, IL-6 (**supplementary Fig. 3**). Similarly, dicarboxylic acids (DCAs), key products of  $\omega$ -fatty oxidation that were strongly associated with rapid agers were positively associated with MCP-1 and IL-6 (**supplementary Fig. 4**). An enrichment of correlated metabolites with these secretory factors suggest a synergistic interaction between senescence-associated secretome, metabolism and biological aging.

### **Metabolites display sexual dimorphism independent of biological age.**

Several factors can influence biological age, one such is gender. It is well known that life expectancies for women are usually higher than men<sup>37,38</sup>. Here we probed the metabolome of our study cohort to understand the implications of sexual dimorphism in biological aging. Consistent with the previous reports<sup>39</sup>, there was a clear metabolomic difference between the males and females in the SOLVE-IT cohort (Fig. 5a). Among females, sphingomyelins were significantly increased compared to males. Similarly, the levels of one of the major endocannabinoids, arachidanoyl glycerol and its precursor stearoyl arachidanoyl glycerol were higher in females (Fig. 5b). On the other hand, as expected in males, the male hormone, androgen-derived metabolites such as androstenediol disulfate (1), androstenediol monosulfate, androstenediol disulfate (2) were found to be elevated. Examining the SASP and proinflammatory factors, it was clear that matrix metalloproteinase (MMP-1) and plasminogen activator inhibitor-1 (PAI-1) were significantly increased in females compared to males. Taking our previous results into consideration (Fig. 4a), we observed that irrespective of the gender, both CCL-2/MCP-1, and Cystatin C were unaltered suggesting biological aging-associated senescence may not be influenced by gender. Interestingly, we did not see any significant differences among the proinflammatory markers in both the sexes (Fig. 5d).

Next, we sought to understand the impact of gender in biological age-associated metabolic signatures (Fig. 5e). For this, we compared the ROC curves of males versus females in predicting healthy and rapid agers. This enables a direct comparison between the sexes by factoring age groups but without

Loading [MathJax]/jax/output/CommonHTML/jax.js analysis. The analysis identified four groups of metabolites:



Cluster I- metabolites that were elevated in *male rapid* agers, but lower in *female rapid* agers (Male  $AUC_{comb} < 0.5$  and female  $AUC_{comb} > 0.5$ , upper left quadrant); Cluster II- metabolites elevated in *healthy* agers of both the sexes (Male  $AUC_{comb} > 0.5$  and Female  $AUC_{comb} > 0.5$ , upper right quadrant); Cluster III- metabolites elevated in *male healthy* and *female rapid* agers (Male  $AUC_{comb} > 0.5$  and female  $AUC_{comb} < 0.5$ , lower right quadrant) and Cluster IV- metabolites elevated in *rapid* agers of both the sexes (Male  $AUC_{comb} < 0.5$  and Female  $AUC_{comb} < 0.5$ , lower left quadrant). A total of 113 metabolites were identified, with 57 metabolites mapping to Cluster 1 (*male rapid* agers, linked to *female healthy* agers). Six acetylated metabolites namely, N2-acetyl, N6-methyllysine, N2-acetyl, N6, N6-dimethyllysine, N-acetylcitrulline, N-acetyl phenylalanine, N-acetylarginine, N-acetyl-3-methylhistidine belonged to Cluster I. Likewise, very-long-chain ( $C > 22$ ) acylcarnitines such as nervonoylcarnitine, cerotoylcarnitine, behenoylcarnitine, ximenoylcarnitine correlated remarkably well with female healthy agers but not with male healthy agers. However, long chain acylcarnitines ( $18 \leq C \leq 22$ ) were associated with both male and female healthy agers. This suggests that even though acylcarnitines are universal markers of aging<sup>33</sup>, gender can have a significant impact. Similarly, some *male healthy* aging-associated metabolites (24) were identified with *female rapid* agers. For example, oxidized methionine, methionine sulfone showed the highest difference in the  $AUC_{comb}$  values with 0.70 in males and 0.39 in females. A few amino acid metabolites such as ornithine, 5-(galactosylhydroxy)-L-lysine, C-glycosyltryptophan, 3-methyl glutaryl carnitine, cystathionine, dimethylguanidino valeric acid (DMGV), hydantoin-5-propionate and hydroxyasparagine were also identified with healthy agers in males but not with females.

We identified 16 metabolites that were associated with healthy agers in both males and females but with significant differences in their power of association (Cluster II). The top metabolites in this group were long chain acylcarnitines like octadecanedioylcarnitine, octadecenedioylcarnitine, which are strong predictors of *male healthy* agers but weak predictors of *female healthy* agers. Similarly, gamma-glutamylcitrulline and S-methyl methionine could predict the *male healthy* agers with an  $AUC_{comb}$  value of 0.80 but this value was reduced to 0.61 and 0.63 respectively, in *female healthy* agers. On the other hand, levels of two major glycolytic metabolites; glucose and pyruvate were strong predictors of *male rapid* agers but their predictive power was significantly lower for *female rapid* agers (Cluster IV) (Fig. 5e, **source data**). Overall, these results suggest a decisive role of sexual dimorphism in the metabolism associated with aging. Of note, none of the biomarkers from the healthy aging metabolomic (HAM) index was affected by gender differences, pointing to the robustness of the HAM index in predicting healthy agers.

### Metabolites associated with race.

Another demographic feature that can influence aging is race. There is strong evidence supporting racial differences in health and life expectancies<sup>40</sup>. We wanted to understand the impact of race on biological aging. So, we analyzed the metabolome of African Americans and Caucasians in the 'SOLVE-IT' cohort (**supplementary Fig. 5**). OPLS-DA model showed a marked distinction in the metabolomic profiles of African Americans and Caucasians (Fig. 6a). Top predictive metabolites largely belonged to lipids.

Hydroxyproline, N6-methyl lysine and xenobiotics sulfate of piperine metabolite (2), sulfate of piperine metabolite (3) were also among top metabolite predictors (Fig. 6b). Plasmalogens containing polyunsaturated fatty acids (PUFAs)- arachidonic acid and linoleic acids, as well as, lysoplasmalogens were significantly elevated in the African Americans (Fig. 6c). Plasmalogens are unique glycerophospholipids with a vinyl ether moiety at the sn-1-position of the glycerol backbone and are involved in protecting cells from reactive oxygen species (ROS)-induced damage<sup>41</sup>. Interestingly, some studies have shown lower systemic F2-Isoprostanes (a validated ROS index) in African American population, suggesting lower oxidative stress<sup>42</sup>. Our data suggests, that elevated levels of plasmalogens in African Americans may possibly be linked to their reduced oxidative stress status. We did not observe any significant difference among the SASP factors (Fig. 6d). Interestingly, IL-6 and soluble IL-6 receptor (sIL-6r) levels were significantly increased in African Americans and Caucasians, respectively. IL-6 is a clear marker of inflammation, whereas sIL-6r is associated with percent body-fat composition<sup>43,44</sup> (Fig. 6e). Tryptophan levels were increased in *African American rapid agers* but not altered among *Caucasians*. Similarly, the levels of hydroxy lysine and azelate (nonanedioate; C9), a DCA, were reduced among *African American healthy agers* but significantly increased in *Caucasian healthy agers*. On the other hand, N-acetylcarnosine was increased in *African American healthy agers* but decreased in *Caucasian healthy agers*. Another significantly important metabolite, bromotryptophan was identified with *African American rapid agers* and not among *Caucasians* (Fig. 6e, **source data**). It has been reported that the levels of serum 6-bromotryptophan is a risk factor for chronic kidney disease (CKD) progression<sup>45</sup>. Considering this, rapid agers of the African American descent in this study cohort may be at a higher risk for CKD. These findings suggest that age-associated metabolites may be influenced by race.

### Metabolites associated with smokers.

Biological aging can be influenced by lifestyle choices such as smoking. Cigarette smoke produces numerous (~ 4000) compounds with varying levels of toxicity and is known to increase the risk of COPD, cardiovascular disease and other age-related diseases. Previous studies have established differences in metabolome of smoked and never-smoked individuals<sup>46</sup>. However, the effect of smoking on the metabolites associated with biological age remains unexplored. Therefore, we analyzed the effect of smoking on the metabolome of the SOLVE-IT cohort. Our OPLS-DA analysis demonstrated a moderate separation between the smoked and never-smoked individuals (Fig. 7a). This separation was predominantly due to xenobiotics related to benzoates and caffeine metabolism. Some of the major metabolites in this list includes, 3-methyl catechol sulfate(s), 3-ethyl catechol sulfate(s), and caffeine (Fig. 7b). It is important to note that about 91% of the 'smoked' population had quit smoking (average years since they quit was 31 years). We did not observe any changes in both SASP (Fig. 7c) and proinflammatory markers (Fig. 7d) suggesting a 'prior smoking status' did not induce prolonged low-grade inflammation.

We then compared the impact of smoking on metabolites associated with biological age. Over all 67 metabolites were significantly altered by the smoking status in the context of biological aging. Cyclic

AMP (cAMP) was strongly associated with healthy agers among the smokers but not the never-smokers. cAMP is known to slow aging process by binding to sirtuins 1 and 3<sup>47</sup>. Interestingly, it has been reported that cAMP levels increase during smoking<sup>48</sup>. Therefore, one possible explanation of our data is that the healthy biological aging of some of the smokers in our study cohort may be linked to the increase in their cAMP levels. Similarly, choline, urea, guanidinosuccinate were strongly associated with the healthy agers of smoked population but they were fairly distributed among healthy and rapid agers of non-smokers. Metabolites such as trigonelline, 3-ethylcatechol sulfate and methyl 3-catechol sulfate were elevated among healthy agers of 'never smoked' population but were not observed in the 'smoked' population (Fig. 7e, **source data**). These metabolites are usually from food; but, it is postulated that smoking can enhance its biological conversion<sup>49,50</sup>. Our results indicate that trigonelline, 3-ethylcatechol sulfate and methyl 3-catechol sulfate may not be affected long-term by smoking. Taken together, our results suggest that smoking status possibly affects some metabolites long-term but their effect on biological age is moderate.

## Discussion

Chronological age is the principal risk factor for several chronic diseases. However, at a population level, individuals do not exhibit phenotypic aging at the same rate. Rapid agers display a faster rate of biological or phenotypic aging relative to their chronological age. Detecting a rapid ager early on will not only present intervention opportunities, but also reduce the socio-economic burden on society. In a society with an ever-increasing aging population, it is therefore critical to identify molecular markers that reflect rapid biological aging. However, it is challenging to differentiate biological age from chronological age. Using a unique cohort of chronologically younger, but biologically rapid agers, and vice versa, here we report metabolic biomarkers for rapid and healthy biological aging. We identified a panel of 18 metabolites that could predict healthy agers with AUC = 0.95. This metabolite panel was not affected by demographic factors such as gender, race or smoking status (**supplementary Fig. 6**), which should be contrasted with the availability of other metabolites that do differentiate individuals based on gender (Fig. 5), race (Fig. 6) and smokers from non-smokers (Fig. 7). Additionally, in this study we also examined a SASP and proinflammatory panel to identify markers of biological age. This approach provides a unique molecular fingerprint associated with rapid and healthy aging.

A few aging indicators using 'omics' data have been identified in recent years, but the most accurate way to assess biological age remains unclear. In this study, we have carefully selected a cohort that offers a possible approach to distinguish chronological aging from biological aging. Our groups were clearly separated by chronological age, with all rapid agers between 65–75 years of age and healthy agers over 75 years of age. To the best of our knowledge, this is the first study to use a cohort that has a negative relationship between biological and chronological aging. Although this is unusual in a normal population, this separation allows us to extract out the true metabolic changes that occur during biological aging.

Our study identified that the difference between utilization of the  $\beta$ -oxidation (acylcarnitines) pathway

Loading [MathJax]/jax/output/CommonHTML/jax.js

c acids) has a greater predictive power than the best

individual predictor (eicosenoylcarnitine) for detecting biological age.  $\beta$ -oxidation is the major catabolic pathway by which medium and long chain fatty acids enter mitochondria via carnitine shuttle. The oxidation steps eventually produce acetyl CoA to fuel the TCA cycle and high energy molecules that feed into the respiratory chain. An alternative to  $\beta$ -oxidation is the  $\omega$ -fatty acid oxidation that primarily occurs in microsomes of the ER and generates DCAs. DCAs may conjugate with carnitines and enter mitochondria for completion of oxidation steps. However, the low levels of acylcarnitines among the rapid agers with subsequent increase in DCAs suggests impaired  $\beta$ -oxidation. Our findings indicate that imbalances in the fatty acid oxidation pathways could possibly lead to accelerated aging. Indeed, whether the impairment of  $\beta$ -oxidation or a preference for  $\omega$ -oxidation drives rapid aging needs to be further explored. Several reports in model organisms indicate the importance of fatty acid metabolism in maintaining healthspan and longevity. For example, over-expression of a  $\beta$ -oxidation enzyme, dodecenoyl CoA delta isomerase in *Drosophilla* extended lifespan<sup>51</sup>. Similarly, in *C. elegans* lipid binding protein signaling increases mitochondrial  $\beta$ -oxidation, decreases lipid storage and promotes longevity, thus implying the role of  $\beta$ -oxidation in healthy aging<sup>52</sup>. While  $\omega$ -oxidation is considered to be an alternative to  $\beta$ -oxidation during low carnitine conditions, it is inefficient in the handling of ROS<sup>53</sup>. The enzyme monooxygenase cytochrome P450 involved in  $\omega$ -oxidation is one of the major producers of H<sub>2</sub>O<sub>2</sub> in microsomes and could therefore possibly drive cellular oxidative stress<sup>54</sup> thus contributing to rapid aging.

We combined two powerful techniques of statistical analysis to derive a metabolic index of healthy aging. OPLS-DA has been shown to be an efficient multivariate analytical techniques for the identification of the most important class predictor. However, the OPLS-DA model has to be used with caution<sup>55</sup>. Therefore, we used OPLS-DA for the initial metabolite selection (i.e., feature selection) followed by modeling using LASSO linear regression, thus resulting in a panel of 18 metabolites (generated through several pathways), and which we refer to as the healthy aging metabolic (HAM) index. Two important metabolites involved in the energy production, citrate and isocitrate of the TCA cycle, were predictors of healthy biological aging. The interconversion of citrate to isocitrate is catalyzed by aconitase. Previous reports suggest that aconitase shows a decline with chronological age<sup>56</sup>. Our study suggests that in people who can possibly maintain aconitase activity have improved healthspan. Metabolites involved in carnitine biosynthesis and  $\beta$ -oxidation such as N6,N6,N6-trimethyllysine, a precursor of carnitine and eicosenoylcarnitine (C20:1), a mono-unsaturated fatty acid (MUFA) carnitine, were both strong predictors for healthy biological aging. Subsequently, several lipid biomarkers, such as cortisone and 1-stearoyl-2-docosahexaenoyl-GPE (18:0/22:6), were also identified as strong predictors of healthy aging. 1-stearoyl-2-docosahexaenoyl-GPE is the major reservoir of docosahexaenoic acid (DHA) and DHA deficiency is strongly associated with cognitive decline during aging<sup>57</sup>. In addition to lipids, the other metabolite that is positively associated with healthy biological aging was  $\beta$ -cryptoxanthin, a precursor to vitamin A. Interestingly, lower serum levels of  $\beta$ -cryptoxanthin in the MARK-AGE cohorts was associated with increased risk of cognitive frailty<sup>58</sup>. The HAM index also consists of metabolites with a negative association with healthy aging. For example, among the metabolites with negative coefficients were two of the well-known collagen degradation products, hydroxyproline and prolylhydroxyproline.

Degradation of collagen is one of the pathologies identified with chronological aging<sup>59</sup>. Similarly, pimelate, a DCA, and an intermediate product of  $\omega$ -oxidation was another metabolite that increased in rapid agers. In all, the HAM index strongly predicted healthy biological agers and was not affected by the demographic and lifestyle factors such as gender, race, and smoking status.

The role of fixed factors, such as gender, in aging is well known. However, the effect of gender differences on the age-related metabolite is understudied. Our ROC analysis illustrated the influence of sexual dimorphism on aging. The key result of this analysis is the identification of very long chain acylcarnitines in female healthy agers. Very long chain acylcarnitines are present in peroxisomes and mediate  $\beta$ -oxidation of very long chain saturated fatty acids (VLSFA). Peroxisomes are crucial organelles that govern cell aging by maintaining homeostasis of ROS and metabolic homeostasis<sup>60</sup>. Increase of VLSFA carnitines in female healthy agers suggested active peroxisomal activity which may also aid in longer life expectancies. Supporting this, studies have shown that increased circulating levels of VLSFA reduce the risk of coronary heart disease<sup>61,62</sup>. Accumulation of oxidized proteins increase with chronological aging and it has been shown that gender differences influence the process of protein oxidation during aging<sup>63</sup>. Our results indicate that degraded products of oxidized proteins such as methionine sulfone are higher in healthy male agers, suggesting effective degradation and removal of accumulated oxidized proteins in healthy agers.

Senescence-associated secretory phenotype (SASP) factors are secreted by senescent cells that accumulate with chronological age and drive multiple age-related pathologies<sup>22</sup>. Here we analyzed a spectrum of SASP factors for potential indicators of rapid biological aging. Out of SASP factors analyzed, two were significantly increased in the rapid agers compared to healthy agers, CCL-2/MCP-1 and Cystatin C. CCL-2/MCP-1 is a crucial component of the SASP in some senescent cell types and treatment with a senolytic (intervention to eliminate senescent cells) has been shown to significantly reduce MCP1<sup>64</sup>. Additionally, MCP1 was found to be significantly higher in frail older adults compared to non-frail adults<sup>65</sup>. Our study identified that CCL-2/MCP-1 was strongly associated with several metabolites including two phospholipid classes (PLC); lysophospholipids and diacylglycerols. Consistent with this, lysophosphatidic acid, has been shown to upregulate CCL-2/MCP-1 levels<sup>66</sup>. Our study introduced additional lysophospholipids to this chart, such as lysophosphatidylethanolamine and lysophosphatidylcholine. Similarly, the role of CCL-2/MCP-1 inducing PLC to produce diacylglycerol has been observed in a previous study<sup>67</sup>, suggesting that MCP-1 associated metabolites need to be further examined for their role in biological age.

Cystatin C is a protease inhibitor primarily involved in the pathology of renal dysfunction. Plasma Cystatin C was recently identified as an effective marker in the assessment of kidney function compared to the traditional creatinine<sup>68</sup>. In addition, Cystatin C is associated with, cardiovascular diseases<sup>69</sup>, neurological disorders<sup>70</sup> and cancer<sup>71</sup>. Considering the strong association of Cystatin C with renal dysfunction, increased levels of Cystatin C with rapid aging may suggest underlying renal dysfunction,

senescence. Another interesting observation is the extremely

high correlation of Cystatin C with the various metabolites. For example, given the heterogeneous sample set, the  $R^2$  value of 0.69 between hydroxyasparagine and Cystatin C is very rare among unrelated metabolites. This strong association is indicative of a close biological interaction between two biomolecules. To the best of our knowledge, the direct relationship between Cystatin C and the highly correlated metabolites is not reported in literature. From this panel, C-glycosyltryptophan, pseudouridine, O-sulfotyrosine, N-acetylthreonine, N-acetylserine, N6-carbamoylthreonyladenosine, and N6-acetyllysine were previously reported to be associated with impaired renal function<sup>72</sup>. In addition to these SASP factors, two other proinflammatory factors, IL-6 and CRP, were also increased in rapid agers. The PolSenior study showed the correlation between the two cytokines and chronological age<sup>73</sup>. Recently it was shown that a panel of 7 SASP factors could predict frailty and adverse outcomes in patients, suggesting SASP acts as an indicator of biological age<sup>74</sup>. However, in their study biological age is closely associated with chronological age, suggesting that SASP cannot act solely as an accelerated aging indicator. Our study indicates that although the association of several inflammatory markers with rapid agers confirms their relationship with biological aging, they were not predictive enough to be included in the HAM index. On the other hand, our results suggest a potential interrelationship between senescence-associated secretome, metabolism and biological aging. Further studies would help us understand the mechanistic role of senescence in regulating age-associated metabolites/metabolism.

Our study does have certain limitations, such as the sample size, leading to the well-known “ $n < p$ ” situation. We employed internal cross-validation, which was the best possible technique within the confines of the sample size. However, potential model overfitting cannot be entirely ruled out, therefore, the results need to be further validated in another data set not used in model development. The study design had aimed to maximize the separation between healthy and rapid agers, and the same level of predictive power may not be realized in a general real world older population where many individuals fall somewhere between the two clearly defined groups. Furthermore, our study is cross sectional and may miss positive and negative changes over time that could impact the results in healthy or rapid agers. Nonetheless, the classified groups in the SOLVE-IT study were separated, thus precisely distinguishing rapid and healthy biological aging. Despite the limited number of participants, much of our study demonstrated high statistical validity indicating that the findings may be extrapolated to broader populations. Another potential limitation is that over the counter (OTC) medications might have had an impact on the overall metabolome. In addition, the impact of intestinal microbiome and dietary information can influence the analysis. Any unknown metabolites that were not included in the panel could benefit from the identification of chemical structures to provide new information.

In conclusion, the present findings confirm that individuals showing signs of early or rapid aging have a distinct metabolome compared to healthy agers. We showed that the difference in fatty acid oxidation pathways better represent the biological aging process than any individual metabolic pathway. Our findings suggest that a balance between the two closely related fatty acid oxidation pathways is required in maintaining a healthy biological aging process. If the balance tips towards  $\omega$ -oxidation pathway, a possible disruption in ROS homeostasis can accelerate aging process. However, why and at what point

this balance gets disrupted and whether this is a cause or consequence remains to be addressed. A proposed Healthy Aging Metabolic Index (HAM), an index derived from 18 metabolites distinguishes between healthy and early agers with AUC = 0.95. Each of these metabolites represents individual age-associated pathways, further reinforcing the involvement of a coordinated metabolic network in defining the biological aging rates. Therefore, any therapeutic intervention to enhance the healthy life span of the elderly population should target a combination of metabolic processes rather than a single pathway.

## Materials And Methods

### Participants

The Solve-IT participants were recruited from several sources. Most were recruited through the University of Pittsburgh Claude D. Pepper Older Americans Independence Center, which maintains a registry of more than 2500 older adults who live in the greater Pittsburgh area and are interested in participating in clinical research. Print and radio ads were also used. Respondents were screened with a standardized phone interview. This study was approved by Institutional Review Board of University of Pittsburgh and complies with all relevant ethical regulations. An informed written consent was obtained from all participants. “Rapid” agers were age 65–75 years who could not walk up a flight of stairs or walk for 15 minutes without resting. “Healthy” agers were age 75 years and older who could walk up a flight of stairs or walk for 15 minutes without resting. We excluded participants with a history of a major cancer. Functional assessments on the cohort are further described in <sup>28</sup>

### Cytokine and SASP analysis

CCL-2/MCP-1, IL1 $\alpha$ , MMP1, PAI1, Cystatin C were quantified using multiplex magnetic bead immunoassays (R&D Systems) based on Luminex xMAP multianalyte profiling platform (Luminex® 100/200™ System) according to the manufacturer’s protocol and analyzed on Bio-Rad Bio-Plex Manager 6.1. Cytokine biomarkers analyzed included C-reactive protein (CRP), tumor necrosis factor alpha (TNF $\alpha$ ) and its receptors (TNF $\alpha$ -R1 and TNF $\alpha$ -R2), interleukin 6 (IL-6) and its soluble receptor (sIL-6R), and interleukin 10 (IL-10) as previously described<sup>75</sup>. For all proteins, more than 80% of the samples were within the detectable range. Undetectable targets were replaced with the lowest value for each protein.

**Sample preparation.** Samples were prepared by Metabolon, Inc. using the automated MicroLab STAR® system from Hamilton Company. Briefly, following addition of various internal standards, samples were deproteinated with methanol under vigorous shaking. The resultant extract was divided into five fractions, vacuum dried briefly to remove the organic solvents and stored under the nitrogen.

**Ultrahigh Performance Liquid Chromatography-Tandem Mass Spectroscopy (UPLC-MS/MS):** Mass spectrometry analysis was performed as described earlier. All methods utilized a Waters ACQUITY ultra-performance liquid chromatography (UPLC) and a Thermo Scientific Q-Exactive high resolution/accurate mass spectrometer interfaced with a heated electrospray ionization (HESI-II) source and Orbitrap mass

Loading [MathJax]/jax/output/CommonHTML/jax.js 1. One aliquot was analyzed using acidic positive ion

conditions, using C18 column (Waters UPLC BEH C18-2.1 × 100 mm, 1.7 μm) with a gradient of water and methanol, containing 0.05% perfluoropentanoic acid (PFPA) and 0.1% formic acid (FA). Another aliquot was also analyzed using the same column but with a high organic gradient of methanol, acetonitrile, water, 0.05% PFPA and 0.01% FA. Other two aliquots were analyzed using basic negative ion optimized conditions: 1) using C18 column (Waters UPLC BEH C18-2.1 × 100 mm, 1.7 μm) eluted with gradient of methanol and water containing 6.5 mM Ammonium Bicarbonate at pH 8 2) using a HILIC column (Waters UPLC BEH Amide 2.1 × 150 mm, 1.7 μm) eluted with a gradient consisting of water and acetonitrile with 10 mM Ammonium Formate pH 10.8. Data dependent MS/MS analysis was performed with dynamic exclusion. The scan range varied slightly between methods but covered 70-1000 m/z.

Data processing: mass spec files were analyzed using Metabolon's inbuilt Laboratory Information Management System (LIMS). Compounds were identified by comparison to library entries of purified standards or recurrent unknown entities. Biochemical identifications were based on three criteria: retention index within a narrow RI window of the proposed identification, accurate mass match to the library ± 10 ppm, and the MS/MS forward and reverse scores between the experimental data and authentic standards. Peaks were quantified using area-under-the-curve and corrected for batch variations and normalized to the median value. The missing values were replaced with the lowest value for each sample.

## Statistical analysis

### Correlation matrix and chord diagram:

We computed Spearman's rank correlation coefficients ( $\rho$ ), and false discovery rate (FDR) method to correct  $p$ -values for multiplicity. A threshold of corrected  $p < 0.05$  was used to identify correlations between super pathways. R functions `rcorr` in package `HMISC`, `p.adjust` and `chordDiagram` in `circularize` were used for analysis.

### Orthogonal projection of partial least square discriminant analysis (OPLS-DA)

Data were classified into rapid and healthy agers as described<sup>28</sup> and OPLS-DA modeling included 7-fold cross validation with 200 iteration in each step. Both predictive and orthogonal scores of the best model were extracted and plotted. Metabolites with Variable Importance of the Projection (VIP) score more than 1 was used in subsequent analyses such as the model prediction. For rapid and healthy agers, we used the data set excluding unknown metabolites whereas in other analysis, the entire set of 1327 metabolites were used. Sartorius SIMCA 16.0 software (Sartorius stedim biotech, Goettingen, Germany) was used for analysis.

Receiver Operator Characteristic (ROC) curve analysis: was performed using `roc` function in `pROC` package. We used healthy and rapid agers as the dichotomous dependent variable. Excess of area under the curve (AUC) over 0.5 was interpreted as representing the strength of the association, 95% confidence



bands for AUC were constructed, and bootstrap methods were used for comparison of AUCs. R packages ggplot2 and roc function in fbroc, and roc.test function in pROC package were used for analysis.

### Calculation of $AUC_{comb}$ values.

We first defined healthy agers as cases and rapid agers as controls and calculated the ROC\_AUC values ( $ROC\_AUC_{HA}$ ), then the controls and cases were reversed and the ROC\_AUC values for predicting rapid agers ( $ROC\_AUC_{RA}$ ) was calculated. Since  $ROC\_AUC_{HA} = 1 - ROC\_AUC_{RA}$ , we combined these values into one variable named  $AUC_{comb}$  as follows:

$$AUC_{comb} = \begin{cases} ROC\_AUC_{HA} & \text{if, } ROC\_AUC_{HA} > 0.5 \\ 1 - (ROC\_AUC_{RA}) & \text{if, } ROC\_AUC_{RA} > 0.5 \\ ROC\_AUC_{HA} \text{ or } ROC\_AUC_{RA} & \text{if, } ROC\_AUC_{HA} = ROC\_AUC_{RA} = 0.5 \end{cases}$$

As a result,  $AUC_{comb} > 0.5$  will denote greater predictive power of a metabolite towards healthy agers and  $AUC_{comb} < 0.5$  will denote greater predictive power towards rapid agers and  $AUC_{comb} = 0.5$  indicates no predictive capacity.

**Statistical modeling of healthy aging.** 253 known metabolites with  $VIP > 1$  in separating healthy from rapid agers were selected for building a mathematical model of healthy aging. In order to identify a more easily interpretable and a relatively less correlated subset of metabolites we used LASSO linear regression for developing the model. The  $\lambda$  parameter that results in the lowest cross validation error following 10-fold cross validation was chosen to build the model. We used 1000 internal bootstrapping replicates with 5 external bootstrapping cycles. The final model consisted of 18 metabolites including, 1-stearoyl-2-docosahexaenoyl-GPE (18:0/22:6), 3,4-dihydroxybutyrate, 3-hydroxyhexanoylcarnitine, 5-hydroxylysine, 5-oxoproline, beta-cryptoxanthin, citrate, cortisone, eicosenoylcarnitine (C20:1), glucuronate, isocitrate, isoleucine, N6,N6,N6-trimethyllysine, N-acetylaspartate (NAA), N-acetyl-beta-alanine, pimelate (C7-DC), prolylhydroxyproline, and vanillylmandelate (VMA). Using the coefficients from the model we define the healthy aging metabolic index (HAMI) as  $HAMI = \sum_{i=1}^{18} a_i m_i$ , where  $a_1 \dots a_{18}$  are the LASSO coefficients, and  $m_1 \dots m_{18}$  are the concentrations of metabolites as shown in Fig. 3e. R packages elasso and glmnet were used for analysis.

**Pathway enrichment analysis.** The Pubchem ID of significant metabolites and the  $p$ -values were used as the input for the Ingenuity Pathway Analysis (IPA). Pathway-enrichment analysis was performed using Qiagen Ingenuity Pathway Analysis (Qiagen, Redwood city, CA). IPA and interpretation were based on the comprehensive and manually curated content of the Ingenuity Knowledge Base, which organizes biological interactions and functional annotations created from primary literature and public and third-party databases.

The source data underlying Figs. Figures 2b, 4c, 4d, 5e, 6e, 7e are provided within the supplied Source Data file. All data are available from the corresponding author upon reasonable request.

## Code availability

Details of R functions and packages used in this study were described in methods section.

## Declarations

## Author Contributions:

AUG, SLG, NR and SP provided study design. SLG, NR and SP assembled study cohort. SH, TA, SP, GN, AUG acquired, analyzed, or interpreted data. DP and AL helped with running Luminex assays. SP and GN provided feedback on statistical analyses. SH, TA and AUG drafted the manuscript with the help of all co-authors. AUG supervised the study.

## Acknowledgements:

This work was supported in part by the Pittsburgh Claude D. Pepper Older Americans Independence Center (P30 AG024827- Pilot Grant A.U.G.). A.U.G. is supported by R00 AG049126. This project used the UPCI Cancer Biomarkers Facility: Luminex Core Laboratory that is supported in part by award P30CA047904.

## References

1. Lunenfeld, B. & Stratton, P. The clinical consequences of an ageing world and preventive strategies. *Best Pract Res Clin Obstet Gynaecol* **27**, 643–659, doi:10.1016/j.bpobgyn.2013.02.005 (2013).
2. Baker, G. T., 3rd & Sprott, R. L. Biomarkers of aging. *Exp Gerontol* **23**, 223–239, doi:10.1016/0531-5565(88)90025-3 (1988).
3. Franceschi, C. & Campisi, J. Chronic inflammation (inflammaging) and its potential contribution to age-associated diseases. *J Gerontol A Biol Sci Med Sci* **69 Suppl 1**, S4–9, doi:10.1093/gerona/glu057 (2014).
4. Peterson, M. J. *et al.* A Novel Analytic Technique to Measure Associations Between Circulating Biomarkers and Physical Performance Across the Adult Life Span. *J Gerontol A Biol Sci Med Sci* **71**, 196–202, doi:10.1093/gerona/glv007 (2016).
5. 10.1111/j.1532-5415.2006.00745.x  
Walston, J. *et al.* Research agenda for frailty in older adults: toward a better understanding of physiology and etiology: summary from the American Geriatrics Society/National Institute on Aging Research Conference on Frailty in Older Adults. *J Am Geriatr Soc* **54**, 991–1001, doi:10.1111/j.1532-5415.2006.00745.x (2006).

6. Gruenewald, T. L., Seeman, T. E., Ryff, C. D., Karlamangla, A. S. & Singer, B. H. Combinations of biomarkers predictive of later life mortality. *Proc Natl Acad Sci U S A* **103**, 14158–14163, doi:10.1073/pnas.0606215103 (2006).
7. Hannum, G. *et al.* Genome-wide methylation profiles reveal quantitative views of human aging rates. *Mol Cell* **49**, 359–367, doi:10.1016/j.molcel.2012.10.016 (2013).
8. Horvath, S. DNA methylation age of human tissues and cell types. *Genome Biol* **14**, R115, doi:10.1186/gb-2013-14-10-r115 (2013).
9. Levine, M. E. *et al.* An epigenetic biomarker of aging for lifespan and healthspan. *Aging (Albany NY)* **10**, 573–591, doi:10.18632/aging.101414 (2018).
10. Lu, A. T. *et al.* DNA methylation GrimAge strongly predicts lifespan and healthspan. *Aging (Albany NY)* **11**, 303–327, doi:10.18632/aging.101684 (2019).
11. Aviv, A. The epidemiology of human telomeres: faults and promises. *J Gerontol A Biol Sci Med Sci* **63**, 979–983, doi:10.1093/gerona/63.9.979 (2008).
12. Mamoshina, P. *et al.* Machine Learning on Human Muscle Transcriptomic Data for Biomarker Discovery and Tissue-Specific Drug Target Identification. *Front Genet* **9**, 242, doi:10.3389/fgene.2018.00242 (2018).
13. Lehallier, B. *et al.* Undulating changes in human plasma proteome profiles across the lifespan. *Nat Med* **25**, 1843–1850, doi:10.1038/s41591-019-0673-2 (2019).
14. Galkin, F. *et al.* Biohorology and biomarkers of aging: Current state-of-the-art, challenges and opportunities. *Ageing Res Rev* **60**, 101050, doi:10.1016/j.arr.2020.101050 (2020).
15. Aguiar-Pulido, V. *et al.* Metagenomics, Metatranscriptomics, and Metabolomics Approaches for Microbiome Analysis. *Evolutionary bioinformatics online* **12**, 5–16, doi:10.4137/ebo.s36436 (2016).
16. de Cabo, R. & Mattson, M. P. Effects of Intermittent Fasting on Health, Aging, and Disease. *N Engl J Med* **381**, 2541–2551, doi:10.1056/NEJMr1905136 (2019).
17. Hatori, M. *et al.* Time-restricted feeding without reducing caloric intake prevents metabolic diseases in mice fed a high-fat diet. *Cell Metab* **15**, 848–860, doi:10.1016/j.cmet.2012.04.019 (2012).
18. Redman, L. M. *et al.* Metabolic Slowing and Reduced Oxidative Damage with Sustained Caloric Restriction Support the Rate of Living and Oxidative Damage Theories of Aging. *Cell Metab* **27**, 805–815.e804, doi:10.1016/j.cmet.2018.02.019 (2018).
19. Niedernhofer, L. J. *et al.* Nuclear Genomic Instability and Aging. *Annual review of biochemistry* **87**, 295–322, doi:10.1146/annurev-biochem-062917-012239 (2018).
20. Hamsanathan, S. *et al.* Cellular Senescence: The Trojan Horse in Chronic Lung Diseases. *American journal of respiratory cell and molecular biology* **61**, 21–30, doi:10.1165/rcmb.2018-0410TR (2019).
21. He, S. & Sharpless, N. E. Senescence in Health and Disease. *Cell* **169**, 1000–1011, doi:10.1016/j.cell.2017.05.015 (2017).
22. Childs, B. G., Durik, M., Baker, D. J. & van Deursen, J. M. Cellular senescence in aging and age-related disease: from mechanisms to therapy. *Nat Med* **21**, 1424–1435, doi:10.1038/nm.4000 (2015).

23. Zhu, Y. *et al.* The Achilles' heel of senescent cells: from transcriptome to senolytic drugs. *Aging Cell* **14**, 644–658, doi:10.1111/accel.12344 (2015).
24. Guralnik, J. M., Ferrucci, L., Simonsick, E. M., Salive, M. E. & Wallace, R. B. Lower-extremity function in persons over the age of 70 years as a predictor of subsequent disability. *The New England journal of medicine* **332**, 556–561, doi:10.1056/nejm199503023320902 (1995).
25. Studenski, S. *et al.* Gait speed and survival in older adults. *Jama* **305**, 50–58, doi:10.1001/jama.2010.1923 (2011).
26. Perera, S. *et al.* Gait Speed Predicts Incident Disability: A Pooled Analysis. *J Gerontol A Biol Sci Med Sci* **71**, 63–71, doi:10.1093/gerona/glv126 (2016).
27. Afilalo, J. *et al.* Gait Speed and Operative Mortality in Older Adults Following Cardiac Surgery. *JAMA cardiology* **1**, 314–321, doi:10.1001/jamacardio.2016.0316 (2016).
28. Breitbach, M. E. *et al.* Exonic Variants in Aging-Related Genes Are Predictive of Phenotypic Aging Status. *Frontiers in genetics* **10**, 1277, doi:10.3389/fgene.2019.01277 (2019).
29. Fulop, T. *et al.* Aging, frailty and age-related diseases. *Biogerontology* **11**, 547–563 (2010).
30. Pluvinage, J. V. & Wyss-Coray, T. Systemic factors as mediators of brain homeostasis, ageing and neurodegeneration. *Nature reviews. Neuroscience* **21**, 93–102, doi:10.1038/s41583-019-0255-9 (2020).
31. Yuan, Y. *et al.* Regulation of SIRT1 in aging: roles in mitochondrial function and biogenesis. *Mechanisms of ageing and development* **155**, 10–21 (2016).
32. Miura, Y. The biological significance of  $\omega$ -oxidation of fatty acids. *Proc Jpn Acad Ser B Phys Biol Sci* **89**, 370–382, doi:10.2183/pjab.89.370 (2013).
33. Rattray, N. J. *et al.* Metabolic dysregulation in vitamin E and carnitine shuttle energy mechanisms associate with human frailty. *Nature communications* **10**, 1–12 (2019).
34. Sorgdrager, F. J. H., Naudé, P. J. W., Kema, I. P., Nollen, E. A. & Deyn, P. P. D. Tryptophan Metabolism in Inflammaging: From Biomarker to Therapeutic Target. *Frontiers in Immunology* **10**, doi:10.3389/fimmu.2019.02565 (2019).
35. Ognibene, A. *et al.* Cystatin C reference values and aging. *Clinical Biochemistry* **39**, 658–661, doi:https://doi.org/10.1016/j.clinbiochem.2006.03.017 (2006).
36. Lustgarten, M. S. & Fielding, R. A. Metabolites Associated With Circulating Interleukin-6 in Older Adults. *J Gerontol A Biol Sci Med Sci* **72**, 1277–1283, doi:10.1093/gerona/glw039 (2017).
37. Austad, S. N. & Fischer, K. E. Sex Differences in Lifespan. *Cell Metab* **23**, 1022–1033, doi:10.1016/j.cmet.2016.05.019 (2016).
38. Bronikowski, A. M. *et al.* Aging in the natural world: comparative data reveal similar mortality patterns across primates. *Science* **331**, 1325–1328, doi:10.1126/science.1201571 (2011).
39. Darst, B. F., Koscik, R. L., Hogan, K. J., Johnson, S. C. & Engelman, C. D. Longitudinal plasma metabolomics of aging and sex. *Aging* **11**, 1262–1282, doi:10.18632/aging.101837 (2019).

40. Cantu, P. A., Hayward, M. D., Hummer, R. A. & Chiu, C. T. New estimates of racial/ethnic differences in life expectancy with chronic morbidity and functional loss: evidence from the National Health Interview Survey. *J Cross Cult Gerontol* **28**, 283–297, doi:10.1007/s10823-013-9206-5 (2013).
41. Braverman, N. E. & Moser, A. B. Functions of plasmalogen lipids in health and disease. *Biochimica et Biophysica Acta (BBA) - Molecular Basis of Disease* **1822**, 1442–1452, doi:https://doi.org/10.1016/j.bbadis.2012.05.008 (2012).
42. Fearheller, D. L. *et al.* Racial differences in oxidative stress and inflammation: in vitro and in vivo. *Clin Transl Sci* **4**, 32–37, doi:10.1111/j.1752-8062.2011.00264.x (2011).
43. Coe, C. L. *et al.* Population differences in proinflammatory biology: Japanese have healthier profiles than Americans. *Brain Behav Immun* **25**, 494–502, doi:10.1016/j.bbi.2010.11.013 (2011).
44. León-Ariza, H. H., Botero-Rosas, D. A., Acero-Mondragón, E. J. & Reyes-Cruz, D. Soluble interleukin-6 receptor in young adults and its relationship with body composition and autonomic nervous system. *Physiological reports* **7**, e14315, doi:10.14814/phy2.14315 (2019).
45. Tin, A. *et al.* Serum 6-Bromotryptophan Levels Identified as a Risk Factor for CKD Progression. *J Am Soc Nephrol* **29**, 1939–1947, doi:10.1681/asn.2017101064 (2018).
46. Hsu, P. C. *et al.* Metabolomic profiles of current cigarette smokers. *Mol Carcinog* **56**, 594–606, doi:10.1002/mc.22519 (2017).
47. Wang, Z. *et al.* Cyclic AMP Mimics the Anti-ageing Effects of Calorie Restriction by Up-Regulating Sirtuin. *Scientific Reports* **5**, 12012, doi:10.1038/srep12012 (2015).
48. Wong, F. H. *et al.* Cigarette smoke activates CFTR through ROS-stimulated cAMP signaling in human bronchial epithelial cells. *American Journal of Physiology-Cell Physiology* **314**, C118-C134, doi:10.1152/ajpcell.00099.2017 (2018).
49. Wang, Y. *et al.* Untargeted Metabolomics Identifies Novel Potential Biomarkers of Habitual Food Intake in a Cross-Sectional Study of Postmenopausal Women. *The Journal of Nutrition* **148**, 932–943, doi:10.1093/jn/nxy027 (2018).
50. Gu, F. *et al.* Cigarette smoking behaviour and blood metabolomics. *International Journal of Epidemiology* **45**, 1421–1432, doi:10.1093/ije/dyv330 (2015).
51. 10.1155/2012/854502  
Lee, S. H., Lee, S. K., Paik, D. & Min, K. J. Overexpression of fatty-acid- $\beta$ -oxidation-related genes extends the lifespan of *Drosophila melanogaster*. *Oxid Med Cell Longev* 2012, 854502, doi:10.1155/2012/854502 (2012).
52. Ramachandran, P. V. *et al.* Lysosomal Signaling Promotes Longevity by Adjusting Mitochondrial Activity. *Dev Cell* **48**, 685–696.e685, doi:10.1016/j.devcel.2018.12.022 (2019).
53. Wanders, R. J., Komen, J. & Kemp, S. Fatty acid omega-oxidation as a rescue pathway for fatty acid oxidation disorders in humans. *Febs j* **278**, 182–194, doi:10.1111/j.1742-4658.2010.07947.x (2011).
54. Johnson, A. L., Edson, K. Z., Totah, R. A. & Rettie, A. E. Cytochrome P450  $\omega$ -Hydroxylases in Inflammation and Cancer. *Adv Pharmacol* **74**, 223–262, doi:10.1016/bs.apha.2015.05.002 (2015).

55. Ruiz-Perez, D., Guan, H., Madhivanan, P., Mathee, K. & Narasimhan, G. in 2018 *IEEE 8th International Conference on Computational Advances in Bio and Medical Sciences (ICCABS)*. 1–1.
56. Yarian, C. S., Toroser, D. & Sohal, R. S. Aconitase is the main functional target of aging in the citric acid cycle of kidney mitochondria from mice. *Mech Ageing Dev* **127**, 79–84, doi:10.1016/j.mad.2005.09.028 (2006).
57. Cardoso, C., Afonso, C. & Bandarra, N. M. Dietary DHA and health: cognitive function ageing. *Nutr Res Rev* **29**, 281–294, doi:10.1017/s0954422416000184 (2016).
58. Rietman, M. L. *et al.* Antioxidants linked with physical, cognitive and psychological frailty: Analysis of candidate biomarkers and markers derived from the MARK-AGE study. *Mech Ageing Dev* **177**, 135–143, doi:10.1016/j.mad.2018.04.007 (2019).
59. Mays, P. K., McAnulty, R. J., Campa, J. S. & Laurent, G. J. Age-related changes in collagen synthesis and degradation in rat tissues. Importance of degradation of newly synthesized collagen in regulating collagen production. *Biochem J* **276** (Pt 2), 307–313, doi:10.1042/bj2760307 (1991).
60. Titorenko, V. I. & Terlecky, S. R. Peroxisome metabolism and cellular aging. *Traffic* **12**, 252–259, doi:10.1111/j.1600-0854.2010.01144.x (2011).
61. Lemaitre, R. N. *et al.* Circulating Very Long-Chain Saturated Fatty Acids and Heart Failure: The Cardiovascular Health Study. *J Am Heart Assoc* **7**, e010019, doi:10.1161/jaha.118.010019 (2018).
62. Malik, V. S. *et al.* Circulating Very-Long-Chain Saturated Fatty Acids and Incident Coronary Heart Disease in US Men and Women. *Circulation* **132**, 260–268, doi:10.1161/circulationaha.114.014911 (2015).
63. Reeg, S. & Grune, T. Protein Oxidation in Aging: Does It Play a Role in Aging Progression? *Antioxidants & redox signaling* **23**, 239–255, doi:10.1089/ars.2014.6062 (2015).
64. Yousefzadeh, M. J. *et al.* Circulating levels of monocyte chemoattractant protein-1 as a potential measure of biological age in mice and frailty in humans. *Aging Cell* **17**, doi:10.1111/accel.12706 (2018).
65. Yousefzadeh, M. J. *et al.* Circulating levels of monocyte chemoattractant protein-1 as a potential measure of biological age in mice and frailty in humans. *Aging Cell* **17**, e12706, doi:10.1111/accel.12706 (2018).
66. Lin, C. I., Chen, C. N., Chen, J. H. & Lee, H. Lysophospholipids increase IL-8 and MCP-1 expressions in human umbilical cord vein endothelial cells through an IL-1-dependent mechanism. *J Cell Biochem* **99**, 1216–1232, doi:10.1002/jcb.20963 (2006).
67. Bose, S. & Cho, J. Role of chemokine CCL2 and its receptor CCR2 in neurodegenerative diseases. *Archives of Pharmacol Research* **36**, 1039–1050, doi:10.1007/s12272-013-0161-z (2013).
68. Roos, J. F., Doust, J., Tett, S. E. & Kirkpatrick, C. M. Diagnostic accuracy of cystatin C compared to serum creatinine for the estimation of renal dysfunction in adults and children—a meta-analysis. *Clin Biochem* **40**, 383–391, doi:10.1016/j.clinbiochem.2006.10.026 (2007).
69. Go, A. S., Chertow, G. M., Fan, D., McCulloch, C. E. & Hsu, C. Y. Chronic kidney disease and the risks of

doi:10.1056/NEJMoa041031 (2004).

70. Sundelöf, J. *et al.* Serum cystatin C and the risk of Alzheimer disease in elderly men. *Neurology* **71**, 1072–1079, doi:10.1212/01.wnl.0000326894.40353.93 (2008).
71. Strojan, P., Oblak, I., Svetic, B., Smid, L. & Kos, J. Cysteine proteinase inhibitor cystatin C in squamous cell carcinoma of the head and neck: relation to prognosis. *Br J Cancer* **90**, 1961–1968, doi:10.1038/sj.bjc.6601830 (2004).
72. Niewczas, M. A. *et al.* Circulating Modified Metabolites and a Risk of ESRD in Patients With Type 1 Diabetes and Chronic Kidney Disease. *Diabetes care* **40**, 383–390, doi:10.2337/dc16-0173 (2017).
73. Puzianowska-Kuźnicka, M. *et al.* Interleukin-6 and C-reactive protein, successful aging, and mortality: the PolSenior study. *Immun Ageing* **13**, 21, doi:10.1186/s12979-016-0076-x (2016).
74. Schafer, M. J. *et al.* The senescence-associated secretome as an indicator of age and medical risk. *JCI Insight* **5**, doi:10.1172/jci.insight.133668 (2020).
75. Langmann, G. A. *et al.* Inflammatory Markers and Frailty in Long-Term Care Residents. *Journal of the American Geriatrics Society* **65**, 1777–1783, doi:10.1111/jgs.14876 (2017).
76. DeLong, E. R., DeLong, D. M. & Clarke-Pearson, D. L. Comparing the areas under two or more correlated receiver operating characteristic curves: a nonparametric approach. *Biometrics* **44**, 837–845 (1988).

## Figures

Figures

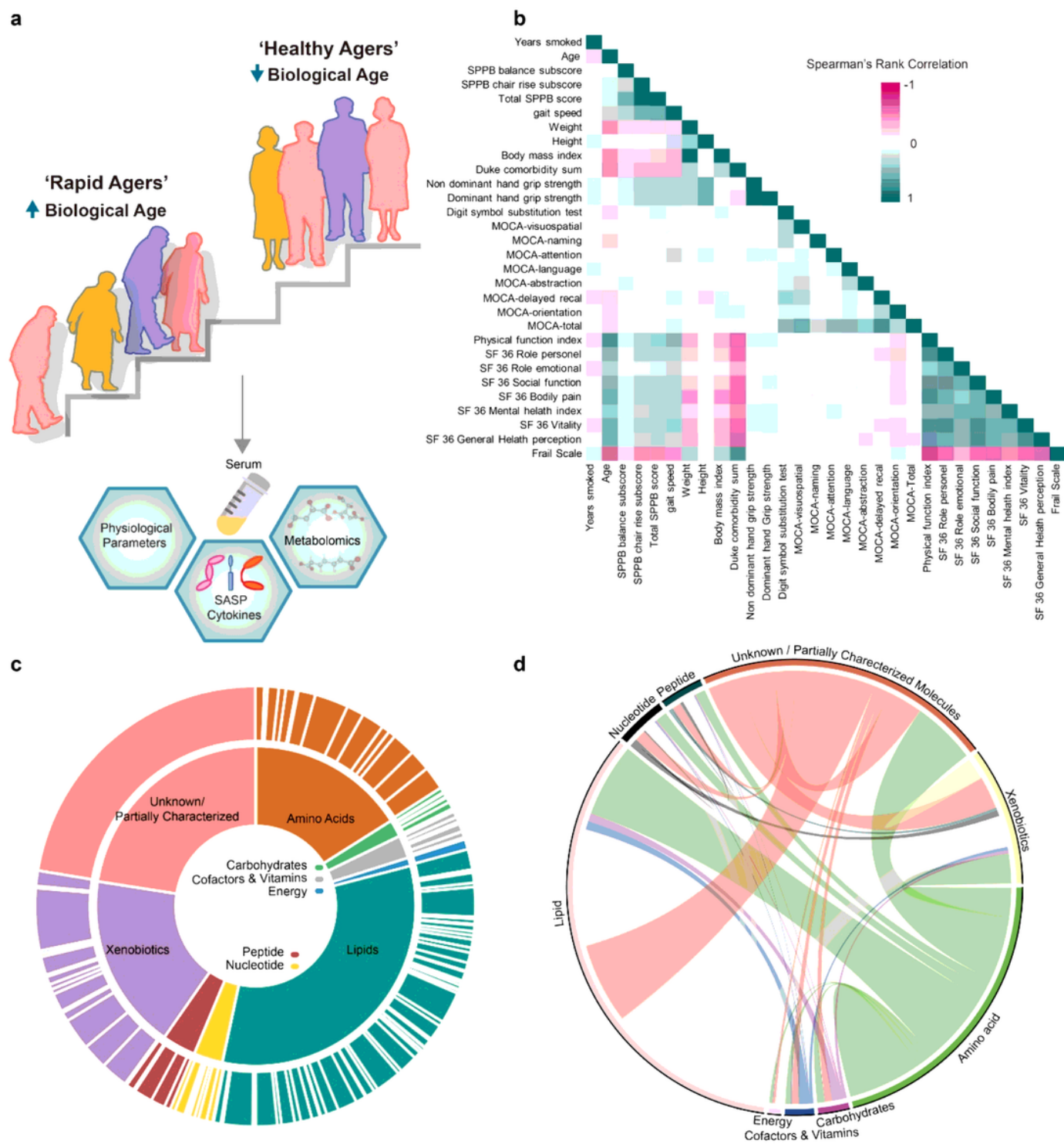


Figure 1

Global metabolic profiling of SOLVE-IT study cohort. a. Study design: A total of 196 participants were recruited through the Claude D. Pepper Older Americans Independence Center at University of Pittsburgh. All study participants were medically-stable volunteers who were independently mobile. Both groups were controlled for demographic and clinical features. Using their performance-based mobility measures, the participants were grouped as “rapid” or “healthy” agers. Serum metabolite profiling was performed using

Loading [MathJax]/jax/output/CommonHTML/jax.js



high resolution LC-MS/MS-based untargeted metabolomics analysis. SASP was measured by Luminex High Performance Assay and proinflammatory markers were measured as previously described<sup>75</sup>. The data from clinical features of phenotypic aging, SASP, cytokines and metabolites were integrated using statistical approaches to generate a molecular index for Biological Aging. b. Heat map shows the Spearman's rank correlations ( $\rho$ ) among the demographic and clinical parameters of the SOLVE-IT cohort. Teal indicates positive and Pink indicates negative associations. MOCA – Montreal Cognitive Assessment; SF-36 – Short Form 36. c. Stacked donut chart showing the distribution of metabolites in super (inner donut) and sub metabolic (outer donut) pathways as identified in KEGG (refer supplementary table 1). d. Number of connections deemed important (FDR corrected p-value for  $p < 0.2$ ) between the metabolites is highlighted in the chord diagram. The thickness of the chord is proportional to the number of relationships.

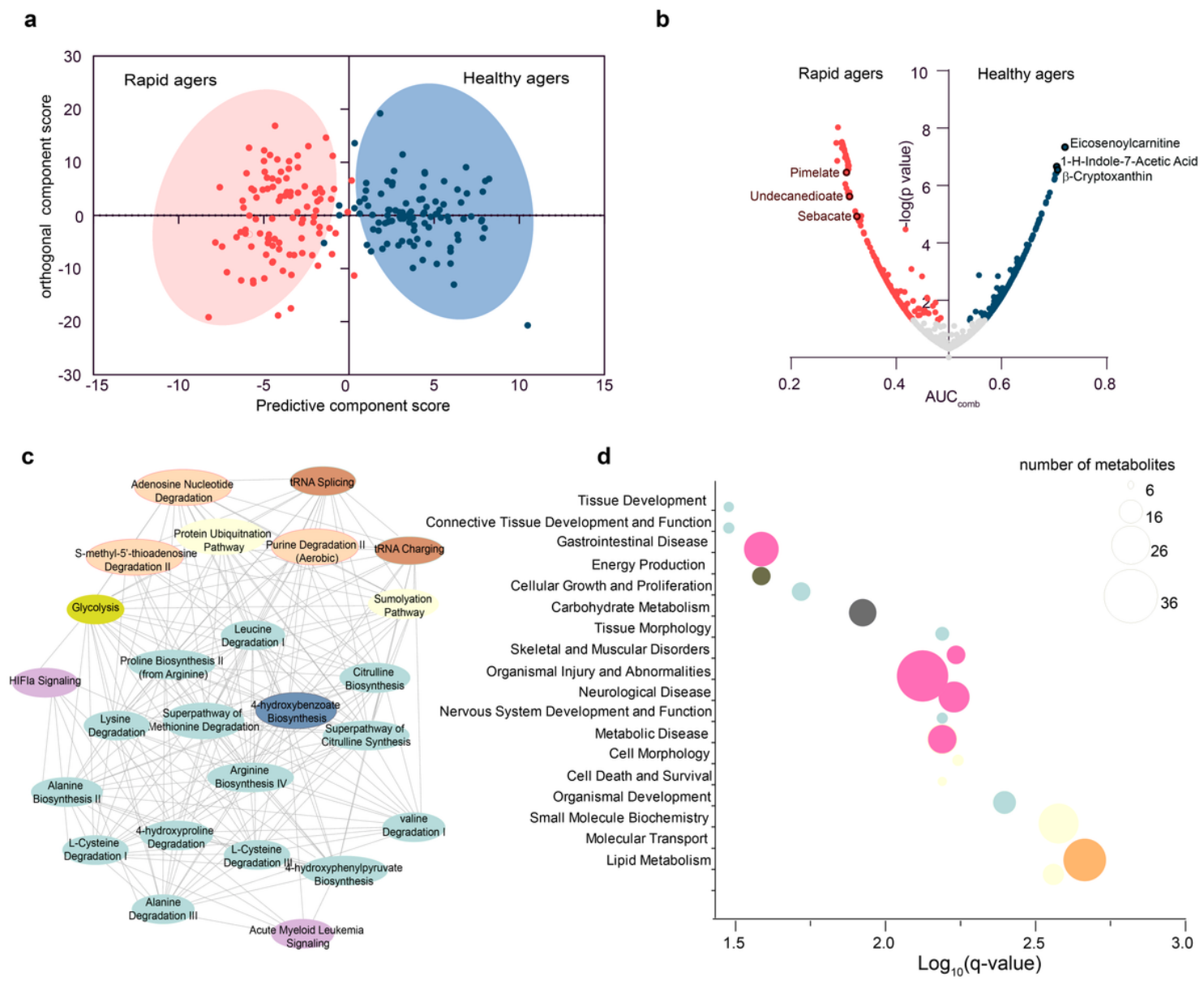
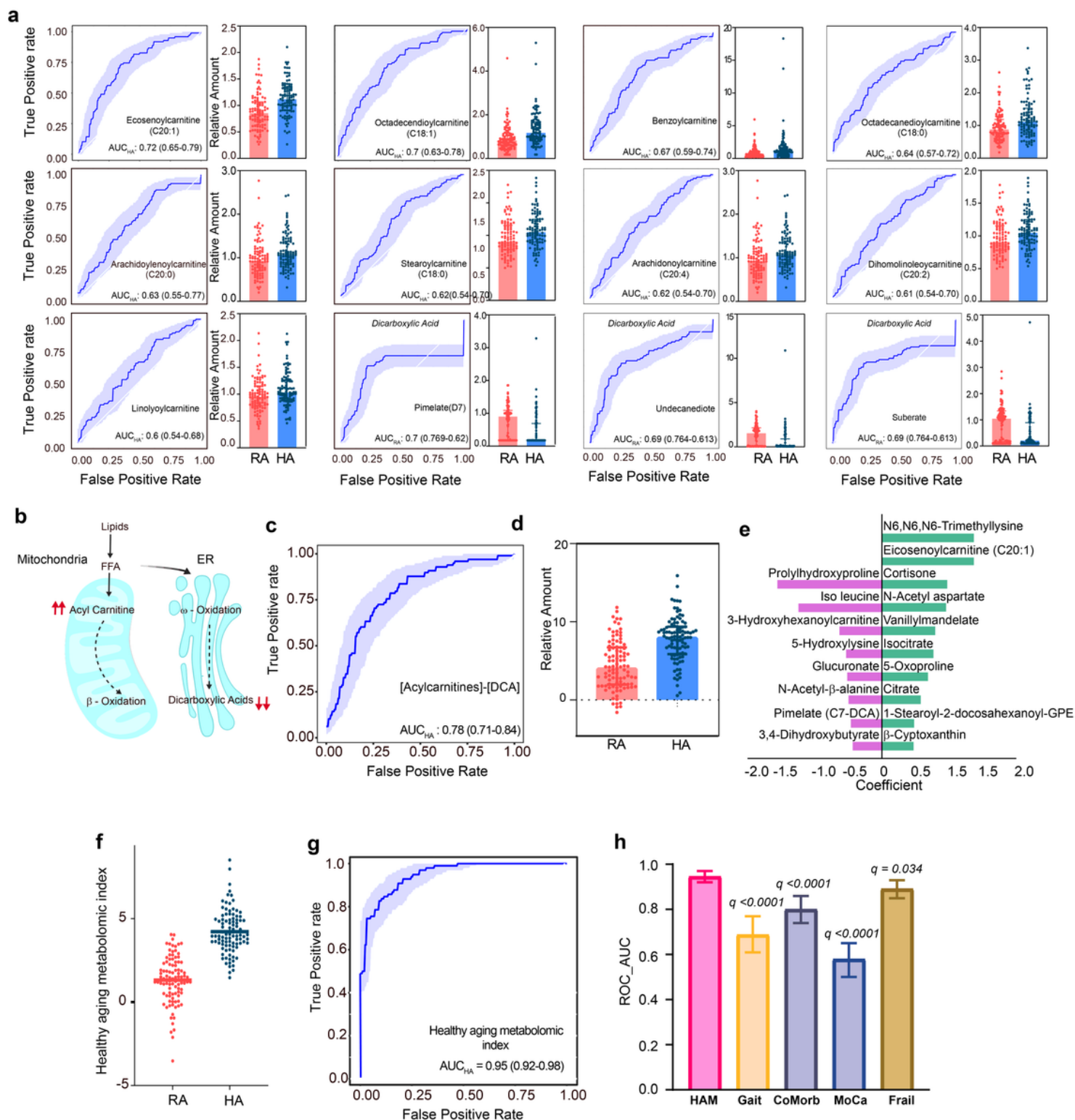


Figure 2

Metabolomic differences between healthy and rapid agers. a. Difference in metabolomic profiles between healthy and rapid agers as evidenced from Orthogonal partial least square-discriminant analysis (OPLS-DA) score plot. b. Receiver operating curve analysis (ROC) was performed to identify metabolites associated with healthy and rapid agers. Metabolites with AUCcomb (combined area under the curve) value  $>0.5$  and adjusted  $q < 0.05$  were predictive of healthy agers, whereas metabolites with an AUCcomb  $< 0.5$  and  $q < 0.05$  were predictive of rapid agers; grey spots represent non-significant metabolites c. Pathway-enrichment analysis was performed using Qiagen Ingenuity Pathway Analysis (IPA). Network of enriched pathways in rapid agers shows alterations in amino acid (AA) biosynthesis. d. Major disease and biofunction pathways associated with predictors of rapid agers are depicted in the bubble plot. Pathways are represented in y-axis and the size of the bubble indicates the number of metabolites identified in each pathway. The q-values were obtained following Benjamini-Hochberg correction of p-values.



**Figure 3**

Identification of Healthy Aging Metabolic (HAM) Index. a. ROC curves for acylcarnitines and dicarboxylic acids (DCA) and their distribution profile in healthy (HA) and rapid agers (RA). Acylcarnitines are increased in healthy agers whereas dicarboxylic acids are decreased. AUCHA =AUC value of ROC curve generated for HA (RA as controls); AUCRA =AUC value of ROC curve generated for RA (HA as controls). b. Loading [MathJax]/jax/output/CommonHTML/jax.js × lipids are substrates for fatty acid oxidation pathways; β-

oxidation (primarily in mitochondria) and  $\omega$ -oxidation (microsomes, ER). The FFA are shuttled into mitochondria via acylcarnitines; consequently, increased levels of acylcarnitines indicate active  $\beta$ -oxidation. Similarly, DCAs are intermediary products of  $\omega$ -oxidation and can serve as indicators of active  $\omega$ -oxidation. d. ROC curve and distribution of the difference in acylcarnitines and DCAs in healthy and rapid agers. e. List of metabolites and its coefficients identified from the model. Healthy Aging Metabolic (HAM) index, was developed using the model parameters. f. HAM index showed a significant difference between rapid agers and healthy agers g. high predictive power (AUCHA = 0.95). h. The AUC value of HAM index is significantly higher than other physiological aging indices. The AUC values of each physiological aging indices were subjected to pair-wise comparison with the AUC value of HAM index as described in DeLong et al.<sup>76</sup> The number above each bar represents the p-value of the individual physiological aging index's vs. HAM index.

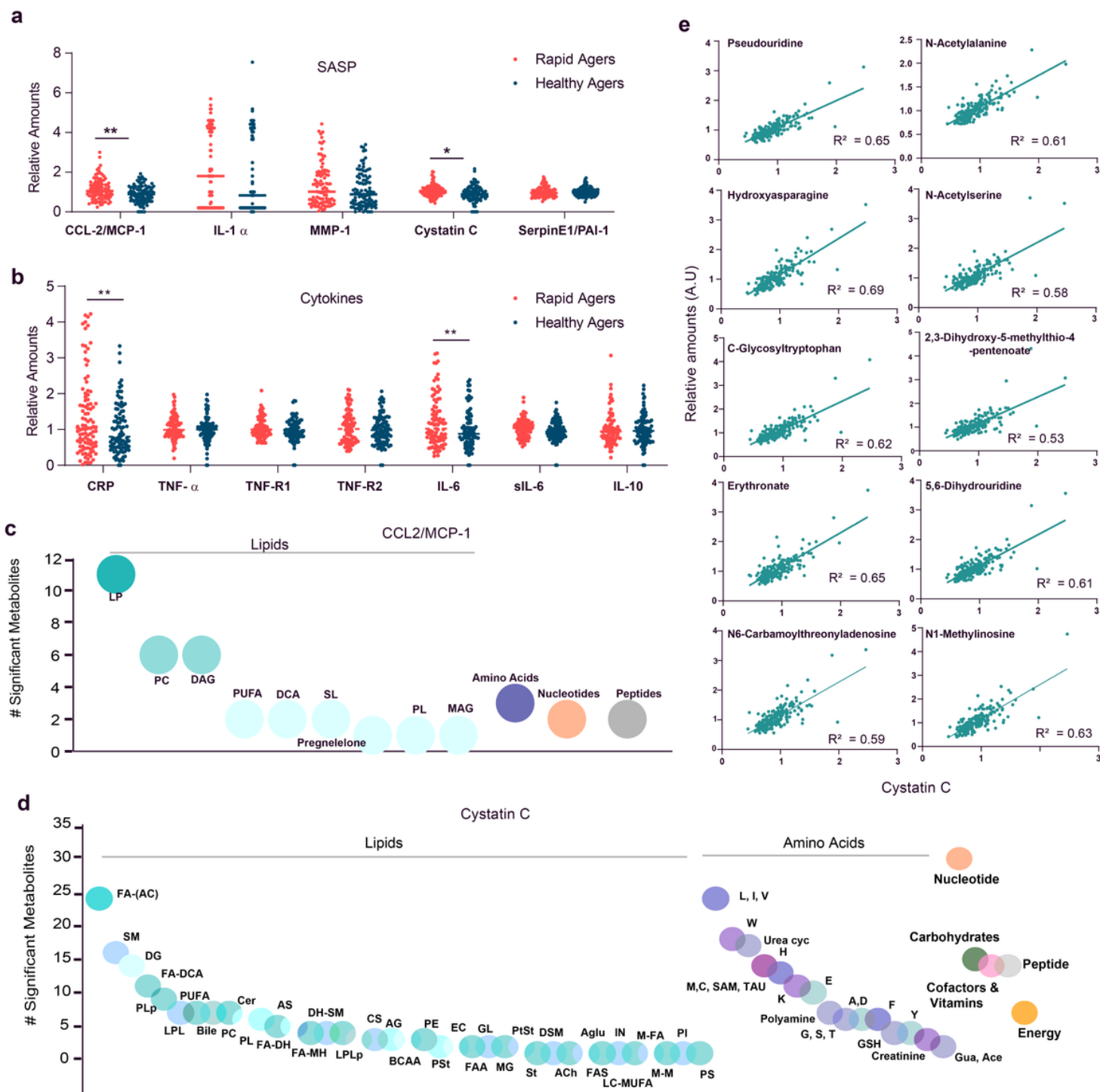


**Figure 4**

Senescence associated secretome linked with biological age. a. Distribution of SASP and b. proinflammatory factors in healthy and rapid agers. CCL2/MCP-1, Cystatin C, CRP and IL-6 levels were increased in rapid agers compared to healthy agers. Bonferroni corrected  $p < 0.05 = *$ ;  $p < 0.01 = **$ . c-d. The number of metabolites significantly associated with each super pathway are represented as bubble plots for c. CCL2/MCP-1 and d. Cystatin C. Lipids were further divided into its sub pathways in both c. and d. Amino acids were further classified in d. Metabolites with  $FDR > 0.2$  for partial Spearman's  $\rho$  controlling for

age and gender were designated as significantly correlated metabolites. e. Scatter plot displaying the top 10 highly correlating metabolites with Cystatin C ( $R^2>0.5$ ).

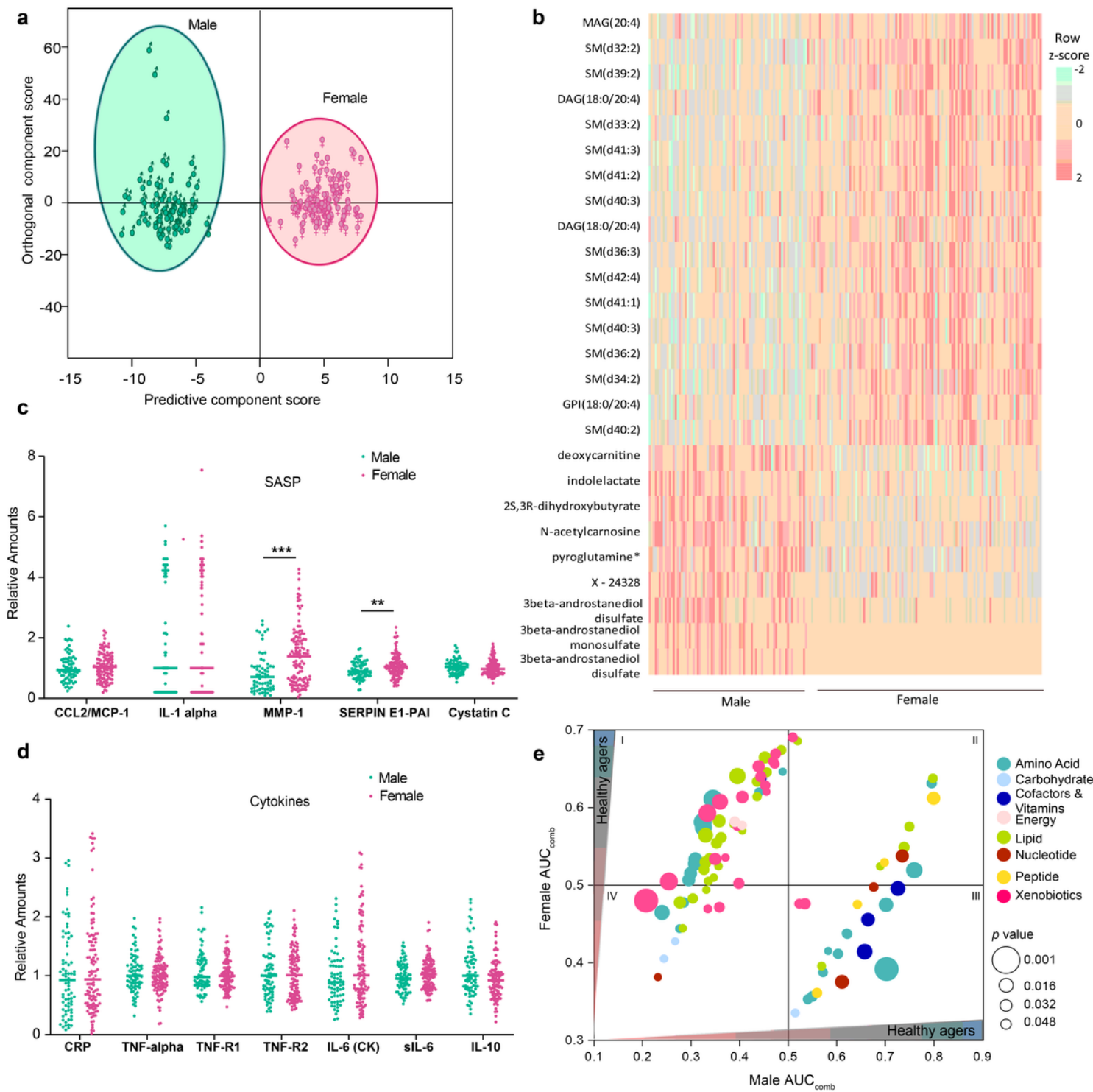
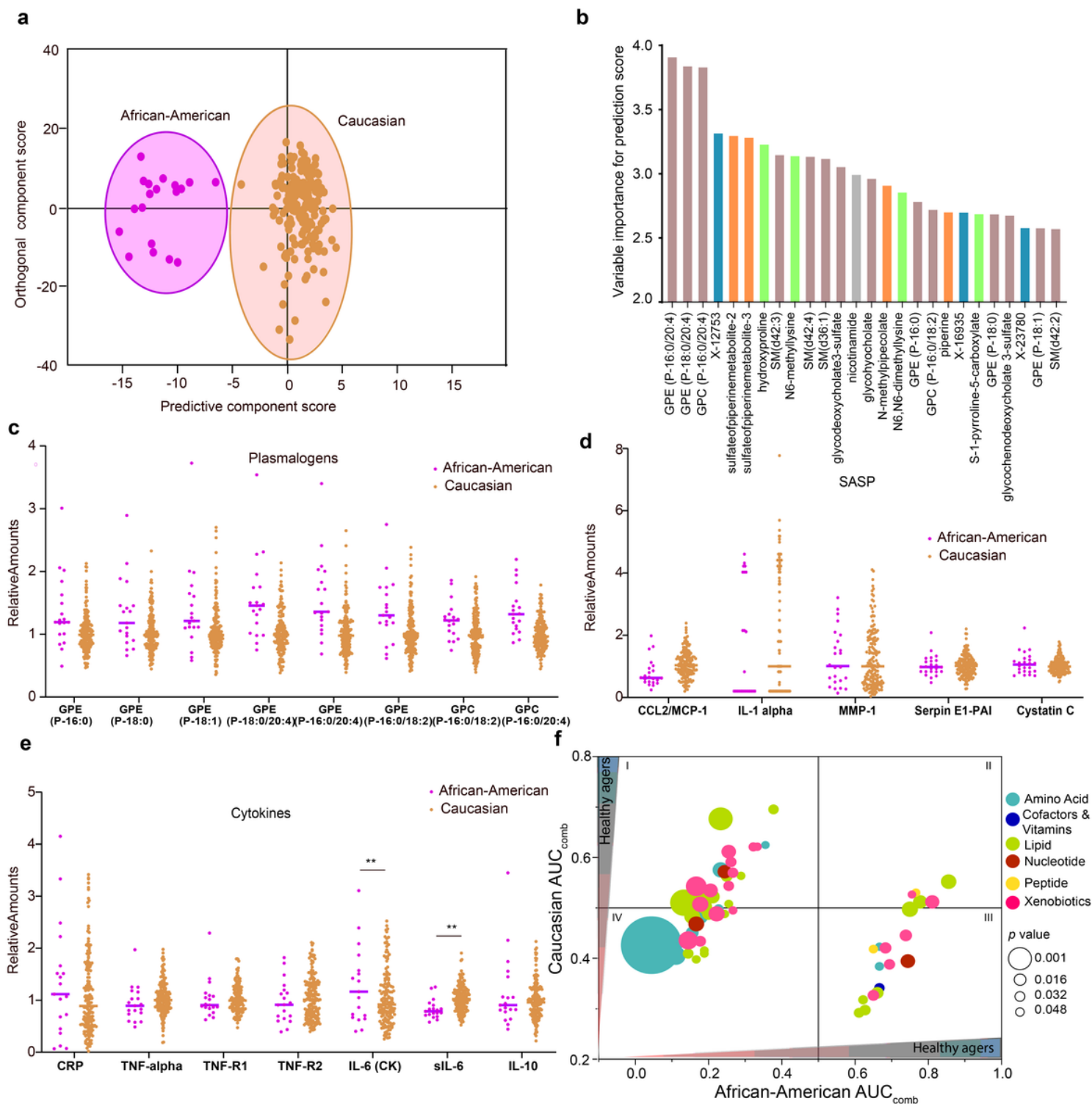


Figure 5

Sexual dimorphism in aging. a. OPLS-DA score plot showing the class separation between males and females in the study population. The separation along predictive axis indicates metabolic distinction between the two groups. b. The top 2 percentile metabolites identified from the OPLS-DA analysis are represented as a heatmap. A dot plot distribution of c. SASP and d. proinflammatory factors in male and

female population. Bonferroni corrected  $p < 0.01 = **$ ;  $p < 0.001 = ***$  e. Bubble plot showing the AUCcomb of metabolites that significantly differ between male and female groups in predicting healthy agers. AUCcomb > 0.5 values = healthy agers, AUCcomb < 0.5 values = rapid agers. Metabolites are color coded based on their super pathways and the sizes represent the p-value. Cluster I: metabolites elevated in female-healthy agers but decreased in male-healthy agers. Cluster II: metabolites elevated in healthy agers of both genders. Cluster III: metabolites that were elevated in female- and male-rapid agers. Cluster IV: metabolites that were decreased in female-rapid agers but increased in male-rapid agers. The ROC curves of metabolites were compared using bootstrap method. Significant metabolites ( $p < 0.05$ ) were plotted.





**Figure 6**

Race-specific changes in metabolites and senescence associated secretome. a. A clear segregation between African-American and Caucasian population is shown in the OPLS-DA score plot and b. the top predictive metabolites that differentiate the two ethnicities is represented as a bar chart. The major group of metabolites belonged to plasmalogens (light brown). c. The distribution of different plasmalogen species are represented. q-values for all plasmalogen species represented are significant ( $<0.01$ ). Dots

Loading [MathJax]/jax/output/CommonHTML/jax.js

proinflammatory factors in African-American and Caucasian



population. Bonferroni corrected  $p < 0.01 = **$  f. Bubble plot showing the differences in AUCcomb of metabolites from this group in predicting healthy agers.

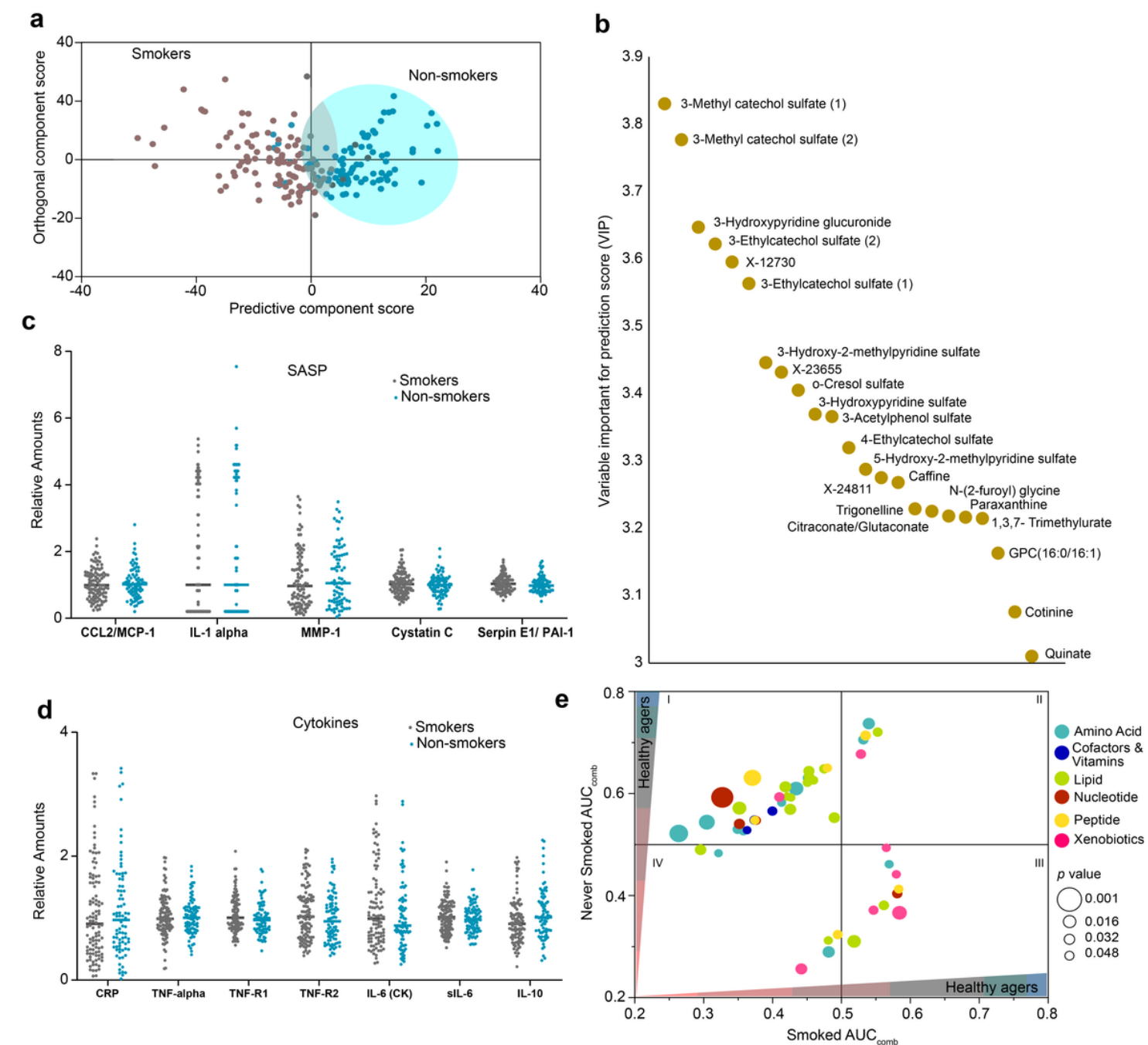


Figure 7

Effect of smoking on biological aging. a. OPLS-DA score plot shows a moderate separation of smokers and non-smokers. b. The top predictive metabolites that differentiate smokers and non-smokers are represented as a dot plot. Most metabolites belonged to xenobiotics. Influence of c. SASP and d. proinflammatory markers in smoking and non-smoking groups are shown as dot plots. e. Differences in AUC of metabolites among the smoking and non-smoking population and its influence on predicting healthy aging is shown as a bubble plot.

## Supplementary Files

This is a list of supplementary files associated with this preprint. Click to download.

- [SuppData.pdf](#)